The regime of aerosol asymmetry parameter over Europe, Mediterranean and Middle East based on MODIS satellite data: evaluation against surface AERONET measurements

M. Korras Carracca[1], N. Hatzianastassiou[2,*], C. Matsoukas[1], A. Gkikas[2], C. D. Papadimas[2]

[1]{ Department of Environment, University of the Aegean, 81100 Mytilene, Greece}

[2]{ Laboratory of Meteorology, Department of Physics, University of Ioannina, 45110 Ioannina, Greece}

Correspondence to: N. Hatzianastassiou (nhatzian@cc.uoi.gr)

Abstract

Atmospheric particulates are a significant forcing agent for the radiative energy budget of the Earth-atmosphere system. The particulates' interaction with radiation, which defines their climate effect, is strongly dependent on their optical properties. In the present work, we study one of the most important optical properties of aerosols, the asymmetry parameter (g_{aer}), in the region comprising of North Africa, the Arabian peninsula, Europe, and the Mediterranean basin. These areas are of great interest, because of the variety of aerosol types they host, both anthropogenic and natural. Using satellite data from the collection 051 of MODIS (MODerate resolution Imaging Spectroradiometer, Terra and Aqua), we investigate the spatio-temporal characteristics of the asymmetry parameter. We generally find significant spatial variability, with larger values over regions dominated by larger size particles, e.g. outside the Atlantic coasts of north-western Africa, where desert-dust outflow is taking place. The g_{aer} values tend to decrease with increasing wavelength, especially over areas dominated by small particulates. The intra-annual variability is found to be small in desert-dust areas, with maximum values during summer, while in all other areas larger values are reported during the cold season and smaller during the warm. Significant intra-annual and inter-annual variability is observed around the Black Sea. However, the inter-annual trends of g_{aer} are found to be generally small.

Although satellite data have the advantage of broad geographical coverage, they have to be validated against reliable surface measurements. Therefore, we compare satellite-measured values with g_{aer} values measured at 69 stations of the global surface AERONET (Aerosol Robotic Network), located within our region of interest. This way, we provide some insight on the quality and reliability of MODIS data. We report generally better agreement at the wavelength of 870 nm (correlation coefficient R up to 0.47), while of all wavelengths the results of the comparison were better for spring and summer.

1 Introduction

Atmospheric aerosol particles interact with radiation, mainly the short wave (SW or solar) part of the spectrum, modifying the energy budget of the Earth-atmosphere system. The aerosol effect is either direct, through the scattering and absorption of solar radiation, and thus reducing the incoming solar radiation flux at the surface, indirect, through the modification of cloud properties, or semi-direct, due to the absorption of solar radiation and consequent modification of the atmospheric temperature profile, convection, and cloud properties (e.g. Graβl, 1979; Hansen, 1997; Lohmann and Feichter, 2005).

The interaction of particles with the solar flux, which defines their climate role, strongly depends on their optical properties (Hatzianastassiou et al., 2004; 2007), which cannot be covered globally by surface in situ measurements. Besides the aerosol optical depth (AOD), which provides a good measure of the aerosol load over an area, one of the most important optical properties of atmospheric particles, which is used in radiative transfer, climate, and general circulation models, is the asymmetry parameter (g_{aer}). The asymmetry parameter describes the angular distribution of the scattered radiation and determines whether the particles scatter radiation preferentially to the front or back. The globally available satellite based AOD data are considered to a great extent reliable and adequate, due to significant developments in surface and satellite measurements during the last two decades, and particularly after 2000. On the other hand, despite of the important role of the asymmetry parameter, relevant global coverage data are measured only for the few last years, or are available in long-term aerosol climatologies such as Global Aerosol Data Set (GADS, Koepke et al. 1997) and Max Planck Aerosol Climatology (MAC, Kinne et al., 2013). Even so, asymmetry parameter data are usually examined for regions with limited geographical extent and temporal coverage (Di Iorio et al, 2003), without intercomparison between alternative data platforms.

The goal of the present work is the study of the spatiotemporal distribution of the aerosol asymmetry parameter, using the most recent data from MODIS (MODerate resolution Imaging Spectroradiometer, collection 051). Emphasis is given to the comparison between the provided MODIS data and respective reliable surface measurements of the global AERONET, in order to gain insight on the quality of the former.

For this study we focus on the region defined by latitudes 5°N to 70°N and longitudes 25°W to 60°E, including North Africa, the Arabian peninsula, Europe, and the greater Mediterranean basin (Fig. 1). This area is selected because of the simultaneous presence of a variety of particles, both natural and anthropogenic (e.g. desert dust, marine, biomass burning, anthropogenic urban / industrial pollution) as shown in previous studies (Lelieveld et al., 2002; Sciare et al., 2003; Pace et al., 2006; Lyamani et al., 2006; Gerasopoulos et al., 2006; Kalivitis et al., 2007). This is due to the fact that two of the largest deserts of the planet are partly included in our area of interest, i.e. the Arabian desert and the Sahara, while one finds also significant sources of anthropogenic pollution, mainly in the European continent, with urban and industrial centres. Moreover, our area of interest and primarily its desert areas, are characterised by a large aerosol load (large optical depth, Remer et al. 2008). Finally, significant regions in this area, more specifically the Mediterranean basin and North Africa, are considered climatically sensitive, since they are threatened by desertification (IPCC, 2007; 2013). This is the first study (to our knowledge) that focuses on asymmetry parameter over a geographically extended area, while at the same time compares satellite with ground-station data.

2 Data

Before presenting the data used in this study a short introduction of the parameter studied is given here for readers more or less unfamiliar with it. The asymmetry parameter (or factor) is defined by:

$$g = \frac{\overline{\omega}_1}{3} = \frac{1}{2}\int_{-1}^{1} P(\cos\Theta)\cos\Theta d\cos\Theta \qquad (1)$$

where P is the phase function, which represents the angular distribution of the scattered energy as a function of the scattering angle Θ and it is defined for molecules, cloud particles, and aerosols, namely our study case. The phase function can be expressed using the Legendre polynomials $\overline{\omega}_l$ (see Liou, 2002) and $\overline{\omega}_1$ in Eq. (1) stands for l=1. The asymmetry parameter is the first moment of the phase function and it is an important parameter in radiative transfer. For isotropic scattering, g equals zero, which is the case for Rayleigh molecular scattering. The asymmetry parameter increases as the diffraction peak of the phase function sharpens. For Lorenz-Mie type particles, namely for aerosols and cloud droplets, the asymmetry parameter takes positive values denoting a relative strength of forward scattering, with increasing values with increasing particle size. It can also take negative values if the phase function peaks in backward directions (90-180°). The phase function along with the extinction coefficient (or equivalently the optical depth) and the single scattering albedo, constitute the fundamental parameters that drive the transfer of diffuse intensity. The asymmetry parameter itself is a simple expression of the phase function (being its first moment) and it is used in many radiative transfer and climate models. Hence, the importance of aerosol asymmetry parameter is easily understood for enabling computations of aerosol radiative properties and effects (e.g. forcings).

Daily data of the aerosol asymmetry parameter (g_{aer}) are used for the needs of this work. In order to achieve the largest geographical coverage of the studied region, we employ satellite data from the MODIS-Terra and MODIS-Aqua datasets. These data are compared with in-situ measurements at stations of the AERONET. We provide a detailed description of the utilised data in the following sections.

2.1 Satellite MODIS Terra and Aqua data

MODIS is an instrument (radiometer) placed on the polar-orbiting satellites of NASA (National Aeronautics and Space Administration) Terra and Aqua, 705 km from the Earth, in the framework of the Earth Observing System (EOS) programme. Terra was launched on 18 December 1999, while Aqua was launched on 4 May 2002. The two satellites are moving on opposite directions and their equatorial crossing times are at 10:30 (Terra) and 13:30 (Aqua). MODIS is recording data in 36 spectral channels between the visible and the thermal infrared (0.44 – 15 μm), while its swath width is of the order of 2330 km, which results in almost full planetary coverage on a daily basis. The global MODIS database is generally considered as one of the most reliable at present.

Aerosol properties are monitored in 7 spectral channels between 0.47 and 2.13 μm and final results are derived through algorithms developed for aerosol quantities both over land and ocean (Kaufman et al., 1997; Tanré et al., 1997; Ichoku et al., 2002; Remer et al., 2005). MODIS data are organised in "collections" and "levels". Collections comprise data produced by similar versions of the inversion algorithms, with the most recent being "051", which includes also outputs from the "Deep Blue" algorithm. Levels are characterised by data of different quality analysis and spatial resolution.

In this study we use daily MODIS data for the asymmetry parameter (g_{aer}) provided on an 1°x1° grid (namely 100x100 km), from the most recent Collection 051, Level 3. These data were measured at wavelengths 470, 660, and 870 nm, only over oceanic regions, since they were derived through the algorithm for aerosol properties over the ocean. The period of analysis stretches from 24-2-2000 to 22-9-2010 for MODIS-Terra and from 4-7-2002 to 18-9-2010 for MODIS-Aqua. We also used Level 3 daily Angström exponent data from MODIS-Aqua C005, and also spectral aerosol optical depth data from MODIS-Aqua C006 datasets, from which we computed C006 Angström exponent. These data were used to assess the validity of g_{aer} data and their changes, as discussed in section 3.2.3.

2.2 Ground based AERONET data

AERONET (AErosol RObotic NETwork) is a global network of stations focused on the study of aerosol properties. AERONET currently encompasses about 970 surface stations (number continuously evolving) equipped with sun photometers of type CIMEL Electronique 318 A (Holben et al., 1998), which take spectral radiation flux measurements.

The optical properties of aerosols are extracted through the application of inversion algorithms (Dubovik and King, 2000). Data are provided on three levels (1.0, 1.5, and 2). In the present work, we use the most reliable Level 2 data, due to their being cloud-screened and quality-assured. AERONET calculates the asymmetry parameter at wavelengths 440, 675, 870, and 1020 nm. We employ daily Level 2 asymmetry parameter data from 69 stations (Fig. 1), contained in our study area (N. Africa, Arabian peninsula, Europe). We choose only coastal stations, in order to maximize the coexistence of satellite marine g_{aer} data with surface data. Also, in order to compare corresponding data between the satellite and station platforms, we perform comparison only for the 440, 675 and 870 nm.

3 Satellite based results

3.1 Geographical distributions

The spatial distribution of annual mean values of g_{aer} is given in Fig. 2 separately at the wavelengths 470, 660 and 870 nm. The values are averages over the common period between Terra and Aqua, namely 4 July 2002 till 18 September 2010. A significant spatial variability is evident, with MODIS-Terra values varying within the ranges 0.63 - 0.76, 0.57 – 0.75, and 0.55 – 0.74, at 470, 660 and 870 nm, respectively. The results exhibit a decreasing tendency of g_{aer} with increasing wavelength, consistent with the theory. Similar results are also obtained from MODIS-Aqua, but with slightly smaller values than Terra by up to 0.02 on average. More specifically, the corresponding ranges of wavelengths are 0.63 - 0.75, 0.57 – 0.73, and 0.55 – 0.73. The smaller Aqua than Terra g_{aer} values could be attributed to smaller sizes of aerosols in midday than morning, corresponding to passages of Aqua and Terra, respectively, associated with lower relative humidity values and shrinking of aerosol particles. Such diurnal variation has been also reported for AOD (Smirnov et al., 2002; Pandithurai et al., 2007), but either decreasing or increasing in the day because of the influence of other factors too, e.g. emissions or wind conditions, apart from aerosol hygroscopicity.

In general, the largest g_{aer} values (deep red colors) are observed off the coasts of West Africa (eastern tropical Atlantic Ocean) at all three wavelengths. High values are also found over the Red and Arabian Seas. These high values are due to strong dust outflows from the Saharan and Arabian deserts carrying out coarse aerosol particles causing strong forward scattering. Nevertheless, the Persian Gulf region, which is surrounded by deserts, is characterized by relatively smaller g_{aer} values. More specifically, values as small as 0.69 (MODIS-Terra) and 0.67 (MODIS-Aqua) are observed in this region at 470 nm, while at the longer wavelengths (660, 870 nm) the smallest values are equal to 0.66 (Terra) and 0.64 (Aqua). The smaller g_{aer} values over the Persian Gulf can be attributed to the presence of fine aerosols, which is corroborated by the low effective radius and large fine-fraction measurements by MODIS over the Persian Gulf, compared to neighbouring areas (not shown here). These fine particles originate from the industrial activities in the Gulf countries related to oilfields or refineries (Goloub and Arino, 2000; Smirnov et al., 2002a,b; Dubovik et al., 2002).

The high g_{aer} values over the northeastern tropical Atlantic Ocean as well as west of the Iberian coasts are possibly related with the presence of coarse sea salt particles. On the other hand, the asymmetry parameter takes clearly smaller values over the Black Sea, where according to MODIS-Terra varies between 0.63 and 0.7 at 470 nm, 0.57 and 0.67 at 660nm, and 0.55 and 0.66 at 870 nm, with the smallest values appearing in the Crimean peninsula (corresponding maximum Aqua values are smaller by 0.02). The small Black Sea g_{aer} values can be associated with the vicinity of industrial but also biomass burning activities in nearby countries. A region of special interest is the Mediterranean basin since it hosts a large variety of aerosols like anthropogenic, desert dust or sea salt (e.g. Barnaba and Gobbi, 2004). The MODIS results over this region show relatively small g_{aer} values, secondary to those of Black Sea, characterized by an increase from north to south, which is more evident at 660 and 870 nm. More specifically, based on MODIS-Terra, g_{aer} over the Mediterranean takes values from 0.68 to 0.74 at 470 nm, while at 670 and 870 nm it ranges from 0.64 to 0.73 and 0.62 to 0.72, respectively. According to MODIS-Aqua the g_{aer} values are slightly smaller again. The observed low values in the northern parts of the Mediterranean are probably associated with the presence of fine anthropogenic aerosols transported from adjacent urban and industrial areas in the north, especially in central Europe. In contrast, the higher g_{aer} values in the southern Mediterranean, particularly near the North African coasts, can be explained by the proximity to the Sahara desert and the frequent transport of significant amounts of coarse dust (e.g. Kalivitis et al., 2006; Hatzianastassiou et al., 2009; Gkikas et al., 2009; 2014).

The spatial distributions of climatological monthly mean g_{aer} values from MODIS-Aqua at 470 nm reveal significant differences either as to the range or to the patterns of the seasonal variability, depending on the area (Fig. 3). Thus, in tropical and sub-tropical areas of Atlantic Ocean (up to about 30°N), where dust is exported from Sahara, g_{aer} keeps high values throughout the year, which reach or even exceed 0.74 locally. Over the regions of Arabian and Red Seas and the Gulf of Aden, which also experience desert dust transport, larger g_{aer} values appear in the period from March to

September, with a maximum on August (locally as high as 0.75-0.76). This seasonal behavior is in line with intra-annual changes of dust production over the Arabian peninsula indicated primarily by MODIS Angström Exponent (AE) and secondarily by Deep Blue aerosol optical depth data and reported in the literature (Prospero et al., 2002). Indeed, the production of dust there is relatively poor in winter, increases in March and April and becomes maximum in June and July (Prospero et al., 2002). Over the Arabian Sea, it is known that large amounts of desert dust are carried out during spring and early summer (Prospero et al, 2002; Savoie et al., 1987; Tindale and Pease, 1999; Satheesh et al., 1999). Nevertheless, according to MODIS, the seasonal variability of g_{aer} remains relatively small there in line with a small seasonal variability in MODIS Deep Blue AE data. This can be explained by the presence of sea salt coarse particles throughout the year, with which dust particles co-exist.

A greater seasonal variability exists over the Persian Gulf, where g_{aer} values are higher during spring and in particular in summer (up to 0.74 at 470 nm according to Aqua), and smaller in autumn and winter (area-minimum values smaller than 0.65). This seasonal behavior can be explained taking into account the meteorological conditions over the greater area of the Gulf; from June to September dry northwestern winds (Shamal) blow from northwest carrying desert dust from the arid areas of Iraq (Heishman 1999; Smirnov et al. 2002a,b). The transport of dust is gradually decreased in autumn, minimizes in winter and increases again in spring. When the presence of desert dust is limited, a significant fraction of total aerosol load in the region is consisted of fine anthropogenic particles (Smirnov et al. 2002a,b), which can explain the observed relatively small g_{aer} values in autumn and winter.

In the Mediterranean basin, g_{aer} exhibits a relatively small seasonal variation, though lower values tend to appear in summer and secondarily in early and late spring, in line with the stronger presence of dust in the area, transported from the Sahara desert (Gkikas et al., 2013). On the contrary, over the Black Sea, a clear seasonal cycle is apparent, with higher values in the cold period of the year and smaller in the warm one. More specifically, according to MODIS-Aqua, the values at 470 nm drop down to 0.61 in summer months whereas they reach 0.7 in January and December.

It is also interesting to look at the geographical distribution of monthly g_{aer} values in latitudes higher than 50°N, for which annual mean values were not given in Fig. 2 because of unavailability of data for all months. Off the coasts of northern France (English Channel) and Germany the asymmetry parameter has small values, with a non-significant annual course (note that values do not exist for January and February). In these areas, the aerosol load consists mainly of anthropogenic polluted particles, which explains the small g_{aer} values there.

In the Baltic Sea (values available from March to October) g_{aer} shows a significant spatial and temporal variability. More specifically, it is small during summer whereas it increases, locally up to more than 0.7, in March and October. The smaller summer values can be explained by the presence of fine aerosols in the Baltic Sea originating from forest fires in Europe and Russia (Zdun et al., 2011). On the contrary, in autumn the local aerosol loading consists largely of coarse marine aerosols . It is also important to note that the Baltic Sea hosts significant amounts of anthropogenic industrial and urban aerosols throughout the year, but especially in summer (Zdun et al., 2011).

In the higher latitudes of Atlantic Ocean, where the presence of maritime aerosols is dominant, it is observed a remarkable month by month variation of asymmetry parameter, with low values in summer (values up to 0.59) against high values (up to 0.75-0.77) in spring (March, April) and autumn (October). This difference is possibly explained by the seasonal variability of aerosol size in the northern Atlantic. Apart from the presence of coarse sea salt throughout the year, in spring and summer small particles are formed through photochemical reactions of dimethylsulphide (DMS) emitted by phytoplankton decreasing the aerosol size. Moreover during summer fine anthropogenic aerosols are transported in the region from North America (Yu, 2003; Chubarova, 2009). These result in lower g_{aer} values between May and August.

Based on MODIS-Terra, the patterns of spatial distribution are generally the same with Aqua, with slightly larger g_{aer} values. At larger wavelengths (660, 870 nm) it is observed a decrease of g_{aer}, in particular of its smallest values. Further details and also an overall picture will be given later on, in the section (3.2.1) which deals with climatological monthly mean values not at the pixel but regional level.

3.2 Temporal variability

3.2.1 Seasonal variability

In order to provide an easier assessment of the seasonal cycle of aerosol asymmetry parameter and its changes from a region to another, but also among the different wavelengths (470, 660 and 870 nm), the study region was divided in 6 smaller sub-regions (see Fig. 1). For each sub-region, the average values of monthly mean climatological data of the pixels found within each sub-region's geographical limits have been computed and are given in Fig. 4, for every wavelength and for Terra and Aqua. It appears that the seasonal cycle differs between the sub-regions, as it has been already shown in the geographical map distributions discussed in the previous section.

At 470 nm (Fig. 4i), the intra-annual variability of g_{aer} is greater over the Black Sea, where it is as large as 0.06 according to MODIS-Terra and 0.05 according to MODIS-Aqua, the north-eastern Atlantic Ocean (0.04 and 0.05 for Terra and Aqua, respectively) and the seas of North Europe (0.05 for both Terra and Aqua). In these regions, there is a tendency for smaller values during summer. More specifically, in the Black Sea the smallest g_{aer} value (0.64) is observed in June, over the seas of North Europe in July and over the north-eastern Atlantic Ocean in August. In these regions, the largest values appear in the cold period of the year. Reverse seasonality with a large seasonal amplitude is observed over the Persian Gulf, where the variability is as large as 0.08, according to both MODIS-Terra and Aqua. The seasonal cycle of g_{aer} over the Middle East exhibits a smaller range of variability (0.02 for MODIS-Terra and 0.03 for Aqua) along with a reverse seasonal variation, with maximum values in summer and minimum in winter. In the other two sub-regions (Mediterranean and eastern Atlantic Ocean) the annual range of values is small (< 0.02). It is noteworthy that in the Mediterranean Sea, there is a weak tendency of appearance of double maxima in winter and spring. The spring maximum should be associated with the presence of desert dust particles, which are transported from Sahara, mainly in the eastern Mediterranean in this season (e.g. Fotiadi et al., 2006; Kalivitis et al., 2007; Papadimas et al. 2008, Gkikas et al. 2009; Hatzianastassiou et al., 2009; Gkikas et al., 2013). There is also a similar transport of Saharan dust in the central and western Mediterranean during summer and autumn (e.g. Gkikas et al., 2009; 2013), but then the predominance is not so clear because of the co-existence of fine anthropogenic aerosols. Regardless of the annual cycle, smaller g_{aer} values are clearly distinguished over the Black Sea and North Europe seas throughout the whole year.

At 660 nm, the g_{aer} values are lower than at 470 nm, in particular over Black Sea, North Europe and North-East Atlantic, whereas the intra-annual variability (range of g_{aer} values) increases up to 0.1 (Terra) and 0.08 (Aqua) over the Black Sea. This increase is mainly attributed to the reduction of summer values due to the strong appearance of fine aerosols in this season. Also, at 660 nm, there is a clearer double annual variation of g_{aer} over the Mediterranean Sea than at 470 nm. At 870 nm the general picture is similar to that of 660 nm though a further increase of month by month variability is noticeable.

In general, our results indicate that over the regions characterized by a strong presence of desert dust particles (eastern Atlantic and the Middle East and Mediterranean Seas) the annual range of variability of g_{aer} is smaller than in the other regions. An additional feature above regions with desert dust is the smaller decrease of g_{aer} values with increasing wavelengths, which can be attributed to the different spectral behavior of solar radiation scattering by fine and coarse aerosols (e.g. Dubovik et al, 2002; J. Bi et al, 2011).

It should be noted here that according to our results, using MODIS-Terra and Aqua data, the g_{aer} seasonal cycle is about similar but with generally greater larger Terra than Aqua values.

3.2.2 Inter-annual variability and changes

Figure 5 displays the geographical distribution of the slope of inter-annual trend of g_{aer} over the study region, as computed from the application of the Mann-Kendall test to time series of deseasonalized monthly anomalies of g_{aer} at 470 nm. Results are shown in units decade^{-1} for both Terra and Aqua over their common time period, namely 2002 – 2010, only if the trend is statistically significant at the 95% confidence level. We also performed the same analysis for the 660 and 870 nm (not shown), with similar results to the 470 nm wavelength.

In general, the estimated changes are relatively small. Terra produces widely statistically significant positive trends, showing that during the period of interest, the asymmetry parameter increased over the examined area, with very few exceptions. The results from Aqua are statistically significant at considerably fewer cells, but also give a few points with decreasing g_{aer}. Based on Terra data, the stronger increases are observed in the eastern and southern Black Sea, as well as over the Baltic and Barents Seas. According to MODIS-Aqua, negative changes are found over few Atlantic Ocean cells. Both Aqua and Terra report increases of g_{aer} over the Persian Gulf, the Red Sea, South Black Sea, East Mediterranean, the coast of the Iberian Peninsula, and some coastal areas of West Africa. The differences encountered between the Terra and Aqua g_{aer} trends may be attributed to the different time of passage of each satellite platform carrying the same MODIS instrument, given that everything else is the same.

Nevertheless, most probably, they may be the result of calibration differences between the two MODIS sensors. It is known that there is a degradation of MODIS sensor (Levy et al., 2010; Lyapustin et al., 2014) impacting time series of MODIS products. More specifically, it is also known that Terra suffers more than Aqua from optical sensor degradation. These calibration issues are known to affect MODIS AOD retrievals, producing an offset between Terra and Aqua, and they are also expected to affect aerosol asymmetry parameter, which is probably more sensitive to such calibration uncertainties that AOD. In this sense, the results of Fig. 5 shown here are not to be taken as truth but rather they are given as a diagnostic of a problematic situation with MODIS aerosol asymmetry parameter inter-annual changes. Such calibration issues are expected to be addressed, at least partly, in the new Collection 006 products. Nevertheless, a preliminary comparison between MODIS Aqua C005 and C006 Angström exponent (AE), which is a common aerosol size parameter, using AE data for the 550-865 pair of wavelengths spanning the period 2002-2010, does not reveal significant modifications in geographical patterns of AE inter-annual changes. This puts some confidence on the C005 g_{aer} results given in the present study. The results of this analysis are presented in detail in the next sub-section (3.2.3).

The overall g_{aer} changes of Fig. 5 may hide smaller timescale variations of g_{aer}, which are obtained by the time-series shown in Fig. 6. Results are given for the 7 sub-regions defined previously, at the three different wavelengths and for Terra and Aqua separately. A general pattern is the decrease of g_{aer} values with increasing wavelength, in particular from 470 to 660 nm. The largest month to month and year to year variation is for Black Sea (Fig. 6i). Relatively large variability is also found in the sub-regions of NE Atlantic (6v), North Europe (6vi) and the Persian Gulf (6vii). On the contrary, small variability is noticed in the eastern Atlantic, where systematic dust outflows from Sahara take place leading to consistently high values of g_{aer}. There are also some other interesting patterns, like the significant drop of g_{aer} with wavelength in areas characterized by the presence of fine aerosols, namely the Black Sea, North Europe and the Persian Gulf (Figs, 6i,vi,vii, respectively). The specific patterns of inter-annual changes of g_{aer} are suggested by both Terra and Aqua, though a slight overestimation by Terra is again apparent in this figure. The obtained results of our analysis are meaningful and in accordance with the theory, underlining the ability of satellite observations to reasonably capture the g_{aer} regime over the studied regions.

3.2.3 Possible uncertainties of MODIS aerosol asymmetry parameter

The MODIS aerosol asymmetry parameter is not a direct retrieval product of the MODIS retrieval algorithm, but it is rather a derived by product. Since this parameter is dependent on aerosol modes used and relative weights, it is understood that there can be uncertainties associated with it. Therefore questions may arise about the validity of g_{aer} and their spatial and temporal patterns presented in the previous sub-sections. Given that, as it was already mentioned, it is an aerosol optical parameter that is valuable and highly required by radiative transfer and climate models, it is worth assessing it through comparison against another more common aerosol size parameter, namely the C005 MODIS Angström exponent at the 550-865 nm wavelength pair ($AE_{550-865}$) over ocean, which is an evaluated MODIS aerosol size product (Levy et al., 2010). Figure 7a, displays the geographical distribution of AE for the study period, i.e. 2002-2010. The main geographical patterns in Fig. 7a are in line with those of asymmetry parameter (Fig. 2). For example, note the high AE values in the Black Sea (yellowish-reddish colors), indicative of fine aerosols, the relatively high values in the Mediterranean Sea (greenish-yellowish colors) and the low values (deep bluish colors) off the western African coasts corresponding to exported Saharan dust. The consistency between g_{aer} and AE data is shown by the strong anti-correlation between the MODIS $AE_{550-865}$ and g_{aer} data at 660 and 870 nm, shown in Figures 7b and 7c, respectively. Strong negative correlation coefficients, larger than 0.7 and 0.8 in Figs 7b and 7c, respectively, relate inversely high/low g_{aer} values with low/high AE ones over the same areas. These results indicate that the spatial patterns of MODIS C005 g_{aer} product are reasonable as compared to the C005 Angström exponent data.

Since questions arise about possible uncertainties regarding the long-term variability of MODIS C005 aerosol size products, due to the calibration issues discussed in the previous section, the corresponding MODIS C006 AE product is displayed in Fig. 8a. From Figs. 8a and 7a a similarity is apparent in the main geographical patterns of the two collections' AE product. The similarity between C005 and C006 AE data is also depicted in the computed correlation coefficients (Fig. 8b), exceeding 0.8, and biases (in absolute and relative percentage terms, Figs 8c and 8d, respectively) which are smaller than 0.1 or 10% in most areas of the study region and 0.2 or 20% almost everywhere. It should be noticed that our AE results are in line with those of Levy et al. (2013, Fig. 15) which refer, however, only to year 2008 (ours are for 2002-2010). In addition, a comparison is attempted in Figs 8e and 8f between the computed trends of C005 and C006 AE data over the common period 2002-2010, in order to assess whether changes are detected, which could be an indication of possible changes in corresponding asymmetry parameter trends. Figures 8e and 8f show the computed deseasonalized trends of slope values for both C005 and C006 AE. The results reveal similar patterns between C005 and C006. Small trends are found in both of them, in agreement with the small trends of asymmetry parameter reported in Fig. 5. It is found that the sign of AE trends mainly does not change from C005 to C006. This might be a signal that no changes of aerosol asymmetry parameter are expected in C006 and puts some confidence on the C005 results given in the present study.

4 Evaluation against AERONET data

In this section, we compare the satellite-measured aerosol asymmetry parameter with measurements from the global network of surface stations of AERONET, which is considered as the reference dataset (Holben et al., 1998). For this purpose, we identified the AERONET stations inside our area of interest and finally utilised only the coastal ones, so that both satellite and surface data be available. The total number of these stations is 69, and their locations are shown in Fig. 1 (blue squares).

Table 1 contains the comparison statistical metrics for all wavelengths (Pearson correlation coefficient, bias, standard deviation, slope, intercept) of the comparison between surface data from AERONET and satellite data from MODIS-Terra and MODIS-Aqua, which correspond to the 1°x1° cell wherein each station is located. For this analysis, we use all cells and days with common data between Terra-AERONET and Aqua-AERONET. The mean differences are calculated as g_{aer}(AERONET)-g_{aer}(Aqua) and g_{aer}(AERONET)-g_{aer}(Terra).

In general, we may note that on an annual level, the MODIS-Terra and Aqua asymmetry parameter values at 470 nm are not in very good agreement with the respective data from AERONET at 440 nm, while the results at the largest wavelengths are more reassuring, though not being very satisfactory (increasing R and decreasing relative bias and RMSE values at 675/660 nm and 870 nm). At 870 nm (Table 1 and Fig. 9), correlation coefficients are found to be the largest and equal to 0.47 (AERONET-Terra) and 0.46 (AERONET-Aqua), while satellite data are slightly overestimated compared to the surface data (bias -0.035 or 5.54% and -0.015 or -2.43%, respectively).

It is important to note that the agreement of satellite and surface data is better in spring and summer, for all studied wavelengths. Specifically, the correlation coefficients increase up to 0.35, 0.50 and 0.54 at 440/470 nm, 660/675 nm and 870 nm, respectively, while the bias decreases down to 0.0005 (0.07%), 0.003 (0.46%) and 0.007 (1.11%), respectively.

Moreover, we find that for all seasons g_{aer} values at 870 nm and 660 nm, both from MODIS-Terra and MODIS-Aqua, are overestimated compared to $g_{aer\ (AERONET)}$ at the corresponding wavelengths (stronger overestimation at 870 nm and by Terra). Finally we note an underestimation of g_{aer} at 470 nm from MODIS-Aqua, relative to the data by AERONET at 440 nm, while very small biases (<0.5 %) are found between Terra and AERONET at the same wavelengths.

In Fig. 9 we present a scatterplot comparison between MODIS and AERONET g data pairs. There is bias towards larger g values from both Aqua and Terra compared to AERONET, with Terra overpredicting more than Aqua. The root mean square error to the fit between MODIS and AERONET is very similar between Aqua and Terra. There are concerns on the application of ordinary least squares regression, arising from the assumption that as the assigned independent variable, AERONET values should be free from error. We cannot guarantee the validity of this assumption, so we recognize that the reported R and slope values from Fig. 9 and Table 1, if viewed as metrics of agreement between MODIS g and real g, may be subject to the effect of regression dilution and consequently biased low. This possible bias for R and slope could be neglected only if AERONET errors can also be considered negligible. With the above caveat in mind, the applied least-squares fit line to the scatterplot comparison between matched MODIS-AERONET data pairs (Fig. 9) indicates that MODIS overestimates g_{aer} more in the smaller than larger values, i.e. more for fine than coarse particles.

We present the frequency distributions of asymmetry parameter daily values (Fig. 10) on the days when data from all three databases (MODIS-Terra, MODIS-Aqua and AERONET) were provided. Fig. 10a corresponds to the whole area of interest, while Figs. 10b and c correspond to two broad sub-regions with basic differences in the aerosol source, namely Europe with great anthropogenic sources, and Africa, Middle East and Arabian peninsula, with predominant natural sources and mainly desert dust. There is an apparent skew in the MODIS-Terra and MODIS-Aqua g_{aer} distributions, while the AERONET distributions are more symmetrical. Moreover, the satellite data distributions show larger values and smaller standard deviations compared to AERONET, with the Terra overestimation being more exaggerated. The disagreement is more pronounced in the sub-region of Europe, while in the sub-region of North Africa / Arabian peninsula, the distributions of satellite and surface data agree more thus confirming the finding of Fig. 9 based on the slope of applied linear regression fit. Values over Europe are generally smaller than over North Africa / Arabian peninsula (Fig. 3), which can be attributed to the presence of larger size particles of desert origin in the latter sub-region, in contrast to Europe, where due to industrial activity and frequent biomass burning the presence of smaller size particles is important. Therefore, the smaller g_{aer} values (<0.6) in the frequency distributions of the whole area, are overwhelmingly contributed by the European sub-region, contrasting with larger values (0.7-0.75) being contributed by both sub-regions and even more by N. Africa/Arabian peninsula at larger g_{aer}.

Potentially useful results may be derived by the comparison of the temporal trends from satellite and surface data. We show in Fig. 11 the absolute and relative changes of the asymmetry factor, calculated through regression on monthly time series of g_{aer} at 9 AERONET stations with satisfactory temporal coverage of data, selected to have recorded at least 40 monthly values. In the same figure, these variations are compared with corresponding data from MODIS-Terra and MODIS-Aqua, from the 1x1 degree cells containing the locations of the 9 selected stations. We note that we only perform this analysis in a month only if all three datasets give data for the specific month. It should be noted that the g_{aer} changes for these stations do not refer to the same period but they all ensure a complete enough time period enabling thus the derivation of safe conclusions on how MODIS and AERONET changes compare to each other. At five out of the nine stations (“Barcelona”, “Dhadnah”, “Lecce University”, “Rome Tor Vergata” and “Villefranche”) the temporal tendencies have the same sign for all three databases, with AERONET showing larger trends. Moreover, the trends are statistically significant at the 95% confidence level for “Barcelona” station.

The overall comparison between satellite and surface g_{aer} data performed in the scatterplot of Fig. 9 and Table 1 does not allow one to have an insight to how the comparison behaves spatially, namely how it differs from a region to another. This is addressed in Fig. 12, showing the comparison of satellite and surface data at the wavelength of 870 nm separately between MODIS-Terra - AERONET and MODIS-Aqua – AERONET. For this comparison, we selected AERONET stations for which there is satisfactory overlap between the time series from AERONET and the time series from MODIS, namely the number of common days between AERONET-Terra and AERONET-Aqua is larger than 100. This intentionally selected less strict criterion that the one used in Fig. 11 is satisfied by 36 stations for AERONET-Terra and by 34 for AERONET-Aqua. For each AERONET station we compute the Pearson correlation coefficient between the station data and the corresponding MODIS-Terra or Aqua data at 870 nm, for the 1°x1° cell containing the station. Moreover, there is the information if the trends between AERONET and either MODIS-Terra or Aqua have the same sign.

In the case of the $g_{aer\ (AERONET)} – g_{aer\ (Terra)}$ comparison, at 5 stations the correlation coefficient R is larger than 0.5, while at 21 stations $0.3<R<0.5$. The largest R found is 0.64 at station “Bahrain”. With respect to the agreement on the sign of the trends, at 24 out of 36 stations (67%) there is a trend sign match and at 12 stations (33%) a mismatch. A similar picture emerges for the comparison $g_{aer\ (AERONET)} – g_{aer\ (Aqua)}$. In this case, there are again 5 stations with $R>0.5$ (maximum value $R=0.61$ again at “Bahrain”), while at 19 stations $0.30<R<0.50$. Also, we see that at 22 stations there is a trend sign match and at 12 there is a mismatch (respective percentages equal to 65% and 35%).

5 Summary and Conclusions

Using satellite data from the latest available collection (051) of MODIS-Terra and Aqua data, we examine the spatiotemporal variations of the aerosol asymmetry parameter over North Africa, the Arabian peninsula and Europe. Generally, the largest values of the asymmetry parameter, indicating the strongest forward scattering of radiation by atmospheric aerosols, are found over areas with aerosol load being dominated by large size particles of desert dust (tropical Atlantic, Arabian and Red Seas),. On the contrary, smaller g_{aer} values are seen where a significant fraction of aerosol load comes from small size particles of anthropogenic origin, e.g. over the Black Sea. The results are consistent with the theory and thus prove a good performance of the MODIS retrieval of aerosol asymmetry parameter. Depending on the area of interest, the seasonal cycle of the asymmetry parameter varies markedly. More specifically, in areas with abundance of desert dust particles, the range of intra-annual variation is small, with the largest values during summer, while in other areas the seasonality is reversed, with the largest values during the cold season and the smallest during the warm season. The asymmetry parameter decreases with wavelength, especially when one examines its spatially minimum values, while this decrease is weaker for the larger g_{aer} values, corresponding to the presence of coarser particles.

The seasonal fluctuation is more pronounced with increasing wavelength in the examined regions, which is attributed to the different spectral behaviour of the asymmetry parameter for small and large particles. With respect to the inter-annual variability of the asymmetry parameter, we did not discern very important either increasing or decreasing tendencies, with absolute changes smaller than 0.04 in any case. On the other hand, we found opposing tendencies for the two satellite datasets. MODIS-Terra observes mostly increasing tendencies, while Aqua gives extensive regions with decreasing tendencies. Generally, the largest intra-annual and inter-annual variations are seen over the Black Sea, while the smallest over the tropical Atlantic. However, some strong trends (especially from Terra) may be due to calibration drift errors, which may be addressed in collection 006. Along these lines we performed some preliminary comparisons between 051 and 006 Angstrom Exponent trends from Aqua, which ensured that AE and g are very closely anti-correlated. These preliminary results, show that 051 Aqua AE trends resemble very closely the 006 trends, supporting that the g trends from collection 051 (at least for Aqua) reported in this study are credible.

We compare satellite data with surface data from the AERONET, in order to validate the reliability of the former. The quantitative comparison is very useful, since satellite data provide broad geographical coverage and are very important in any study related to aerosols and their climate impact. The disagreement with surface stations can give insights in the resulting errors. Through the examination of frequency distributions of daily g_{aer}, a shift of satellite data towards larger values relative to surface data becomes apparent. This finding is more pronounced for g_{aer} over Europe, while the North African, Arabian peninsula values are more in agreement. Moreover, the smallest g_{aer} values originate from particles from Europe, because of the generation of smaller size particles by industrial activities and biomass burning.

In this work we present scatter plots of daily g_{aer} values between MODIS-Terra, MODIS-Aqua, and AERONET, which show moderate agreement between satellite data at 470 nm and surface data at 440 nm, with small correlation coefficients ($R<0.3$). Slightly better agreement was noted at larger wavelengths, but still without reaching very satisfactory levels ($R<0.47$). Nevertheless, during spring and summer, satellite and surface measurements tend to agree more. Finally, for the comparisons at 660/675 and 870 nm, we report an overestimation of g_{aer} by MODIS compared to

AERONET, as expected because of the less steep decrease of g_{aer} with wavelength of MODIS.

We extract pairs of daily Terra-AERONET and Aqua-AERONET values at stations with at least 100 common days. At 21 of 36 stations (Terra-AERONET comparison) and at 19 of 34 stations (Aqua-AERONET comparison) we derive $0.3<R<0.5$, while at 5 stations in both cases, the correlation coefficients are larger than 0.5. Finally, as far as the signs of temporal trends are concerned, we determine agreement in 67% (Terra-AERONET comparison) and in 65% of stations (Aqua-AERONET comparison).

The results of the present analysis are useful since they assess for the first time the performance of satellite based products of aerosol asymmetry parameter over broad regions of special climatic interest. Our results can offer an interesting way to assess the uncertainty induced by the use of such satellite g_{aer} data in climate and radiative transfer models that compute aerosol radiative and climate effects. The obtained results are relatively satisfactory given the difficulties encountered by satellite retrieval algorithms due to the different assumptions they made. The identified weaknesses may provide an opportunity to improve such satellite retrievals of aerosol asymmetry parameter in forthcoming data products like those of MODIS C006.

7 Acknowledgments

This research has been co-financed by the European Union (European Social Fund – ESF) and Greek national funds through the operational programme “Education and Lifelong Learning” of the National Strategic Reference Framework (NSRF) – Research Funding Program: THALES. Investing in knowledge society through the European Social Fund. The Collection 005 MODIS-Terra data were obtained from NASA’s Level 1 and Atmosphere Archive and Distribution System (LAADS) website (ftp://ladsweb.nascom.nasa.gov/). We would like to thank the principal investigators maintaining the AERONET sites used in the present work.

References

Barnaba F. and G. P. Gobbi: Aerosol seasonal variability over the Mediterranean region and relative impact of maritime, continental and Saharan dust particles over the basin from MODIS data in the year 2001, Atmospheric Chemistry and Physics, 4, 4285 - 4337, SRef-ID: 1680-7375/acpd/2004-4-4285SRef-ID: 1680-7375/acpd/2004-4-4285, 2004.

Chubarova, N. Y.: Seasonal distribution of aerosol properties over Europe and their impact on UV irradiance, Atmos. Meas. Tech., 2, 593–608, doi:10.5194/amt-2-593-2009, 2009.

Di Iorio, T., A. di Sarra, W. Junkermann, M. Cacciani, G. Fiocco, and D. Fua, Tropospheric aerosols in the Mediterranean: 1. Microphysical and optical properties, J. Geophys. Res., 108(D10), 4316, doi:10.1029/2002JD002815, 2003

Dubovik, Oleg, Brent Holben, Thomas F. Eck, Alexander Smirnov, Yoram J. Kaufman, Michael D. King, Didier Tanré, Ilya Slutsker, 2002: Variability of Absorption and Optical Properties of Key Aerosol Types Observed in Worldwide Locations. *J. Atmos. Sci.*, **59**, 590–608.

Dubovik, O. and M. D. King, 2000: A flexible inversion algorithm for retrieval of aerosol optical properties from Sun and sky radiance measurements," J. Geophys. Res., 105, 20 673-20 696.

Fotiadi, A., E. Drakakis, N. Hatzianastassiou, C. Matsoukas, K. G. Pavlakis, D. Hatzidimitriou, E. Gerasopoulos, N. Mihalopoulos, and I. Vardavas (2006), Aerosol physical and optical properties in the eastern Mediterranean Basin, Crete, from Aerosol Robotic Network data, Atmos. Chem. Phys., 6, 5399– 5413.

Gerasopoulos, E., Kouvarakis, G., Babasakalis, P., Vrekoussis, M., Putaud, J. P., and Mihalopoulos, N.: Origin and variability of particulate matter (PM10) mass concentrations over the Eastern Mediterranean, Atmos. Environ., 40, 4679–4690, 2006.

Gkikas, A., Hatzianastassiou, N., and Mihalopoulos, N.: Study and characterization of aerosol episodes in the Mediterranean basin for the 7-year period 2000–2007 based on MODIS data, European Aerosol Conference, Greece, Thessaloniki, 24–29 August 2008.

Gkikas, A., Hatzianastassiou, N., and Mihalopoulos, N.: Aerosol events in the broader Mediterranean basin based on 7-year (2000–2007) MODIS C005 data, Ann. Geophys., 27, 3509–3522, doi:10.5194/angeo-27-3509-2009, 2009.

Gkikas, A., Houssos, E., Hatzianastassiou, N., Papadimas, C. and Bartzokas, A. (2011), Synoptic conditions favouring the occurrence of aerosol episodes over the broader Mediterranean basin. Q.J.R. Meteorol. Soc.. doi: 10.1002/qj.978

Goloub, P., and O. Arino, 2000: Verification of the consistency of POLDER aerosol index over land with ATSR-2 fire product. Geophys. Res. Lett., 27, 899–902.

Graßl, H.: Possible changes of planetary albedo due to aerosol particles, in Man’s Impact on Climate, edited by: W. Bach, J. Pankrath, and W. Kellogg, Elsevier, New York, 1979.

Hansen, J., Sato, M., and Ruedy, R.: Radiative forcing and climate response, J. Geophys. Res., 102, 6831–6864, 1997.

Hatzianastassiou, N., B. Katsoulis, I. Vardavas: Sensitivity analysis of aerosol direct radiative forcing in ultraviolet - visible wavelengths and consequences for the heat budget, Tellus, 56b, 368 - 381, 2004.

Hatzianastassiou, N., A. Gkikas, N. Mihalopoulos, O. Torres, and B. D. Katsoulis: Natural versus anthropogenic aerosols in the eastern Mediterranean basin derived from multiyear TOMS and MODIS satellite data, J. Geophys. Res., 114, D24202, doi:10.1029/2009JD011982, 2009.

Hatzianastassiou, N., Matsoukas, C., Drakakis, E., Stackhouse Jr., P. W., Koepke, P., Fotiadi, A., Pavlakis, K. G., and Vardavas, I.: The direct effect of aerosols on solar radiation based on satellite observations, reanalysis datasets, and spectral aerosol optical properties from Global Aerosol Data Set (GADS), Atmos. Chem. Phys., 7, 2585-2599, doi:10.5194/acp-7-2585-2007, 2007.

Haywood, J.M., and O. Boucher, 2000: Estimates of the direct and indirect radiative forcing due to tropospheric aerosols: A review.Rev. Geophys., 38, 513–543.

Heishman, J. (1999), Commanding Officer, Forecaster's Handbook, U.S. Navy Cent. Meteorol. and Oceanogr. Cent., Manama, Bahrain.

Holben B.N., T.F. Eck, I. Slutsker, D. Tanré, J.P. Buis, A. Setzer, E. Vermote, J.A. Reagan, Y. Kaufman, T. Nakajima, F. Lavenu, I. Jankowiak, and A. Smirnov, 1998: AERONET - A federated instrument network and data archive for aerosol characterization, Rem. Sens. Environ., 66, 1-16.

Ichoku C., D. Allen Chu,Shana Mattoo,Yoram J. Kaufman, Lorraine A. Remer, Didier Tanre´, Ilya Slutsker, and Brent N. Holben: A spatio-temporal approach for global validation and analysis of MODIS aerosol products. GEOPHYSICAL RESEARCH LETTERS, VOL. 29, NO. 12, 10.1029/2001GL013206, 2002.

IPCC, 2007: Climate Change 2007: The Physical Science Basis. Contribution of Working Group I to the Fourth Assessment Report of the Intergovernmental Panel on Climate Change [Solomon, S., D. Qin, M. Manning, Z. Chen, M. Marquis, K.B. Averyt, M.Tignor and H.L. Miller (eds.)]. Cambridge University Press, Cambridge, United Kingdom and New York, NY, USA.

IPCC, 2013: Climate Change 2013: The Physical Science Basis. Contribution of Working Group I to the Fifth Assessment Report of the Intergovernmental Panel on Climate Change [Stocker, T.F., D. Qin, G.-K. Plattner, M. Tignor, S.K. Allen, J. Boschung, A. Nauels, Y. Xia, V. Bex and P.M. Midgley (eds.)]. Cambridge University Press, Cambridge, United Kingdom and New York, NY, USA, 1535 pp.

Jianrong Bi, Jianping Huang, Qiang Fu, Xin Wanga, Jinsen Shi , Wu Zhang , Zhongwei Huang, Beidou Zhang: Toward characterization of the aerosol optical properties over

Loess Plateau of Northwestern China. Journal of Quantitative Spectroscopy & Radiative Transfer 112 (2011) 346–360

Kalivitis, N., Gerasopoulos, E., Vrekoussis, M., Kouvarakis, G., Kubilay, N., Hatzianastassiou, N., Vardavas, I., and Mihalopoulos, N.: Dust transport over the eastern Mediterranean derived from TOMS, AERONET and surface measurements, J. Geophys. Res., 112, D03202, doi:10.1029/2006JD007510, 2007.

Kaufman, Y. J., D. Tanré, L. A. Remer, E. F. Vermote, A. Chu, and B. N. Holben: Operational remote sensing of tropospheric aerosol over land from EOS moderate resolution imaging spectroradiometer, J. Geophys. Res., 102, 17,051– 17,067, 1997.

Kinne, S., D. O'Donnel, P. Stier, S. Kloster, K. Zhang, H. Schmidt, S. Rast, M. Giorgetta, T. F. Eck, and B. Stevens (2013), MAC-v1: A new global aerosol climatology for climate studies, J. Adv. Model. Earth Syst., 5, 704–740, doi:10.1002/jame.20035.

Koepke, P., M. Hess, I.Schult, and E. P. Shettle: Global aerosol data set, Rep. No. 243, Max-Planck Institut fuer Meteorologie, Hamburg, Germany, 44 pp., 1997.

Lelieveld, J., et al. (2002), Global air pollution crossroads over the Mediterranean, Science, 298, 794– 799, doi:10.1126/science.1075457.

Lohmann U., Feichter, J. [2005] Global indirect aerosol effects: A review . Atmos. Chem. Phys., 5, 715-737

Lyamani, H., F. J. Olmo, A. Alca´ntara, and L. Alados-Arboledas (2006), Atmospheric aerosols during the 2003 heat wave in southeastern Spain. I: Spectral optical depth, Atmos. Environ., 40, 6453 – 6464, doi:10.1016/ j.atmosenv.2006.04.048.

Papadimas, C. D., N. Hatzianastassiou, N. Mihalopoulos, X. Querol, and I. Vardavas (2008), Spatial and temporal variability in aerosol properties over the Mediterranean basin based on 6-year (2000–2006) MODIS data, J. Geophys. Res., 113, D11205, doi:10.1029/2007JD009189.

Pace, G., A. di Sarra, Meloni, D., Piacentino, S., and Chamard, P.: Aerosol optical properties at Lampedusa (Central Mediterranean). 1. Influence of transport and identification of different aerosol types, Atmos. Chem. Phys., 6, 697–713, 2006, www.atmos-chem-phys.net/6/697/2006/.

Pandithurai, R. T. Pinker, P. C. S. Devara, T. Takamura, K. K. Dani, Seasonal asymmetry in diurnal variation of aerosol optical characteristics over Pune, western India, J. Geophys. Res., 112, D8, DOI: 10.1029/2006JD007803, 2007.

Prospero, J., P. Ginoux, O. Torres, and S. E. Nicholson (2002), Environmental Characterization of Global sources of atmospheric soil dust derived from the NIMBUS-7 TOMS absorbing aerosol product, Rev. Geophys., 40(1), 1002, doi:10.1029/20000GR000095.

Remer L.A., Kaufman Y.J., Tanre D. and co-authors: The MODIS aerosol algorithm, products, and validation, J. Atmos. Sci., 62: 947-973, 2005.

Remer LA, Kleidman RG, Levy RC, Kaufman YJ, Tanr'e D, Mattoo S, Martins JV, Ichoku C, Koren I, Yu H, Holben BN. 2008. Global aerosol climatology from the MODIS satellite sensors. Journal of Geophysical Research 113: D14S07, DOI: 10.1029/2007JD009661.

Satheesh, S. K., V. Ramanathan, X. Li-Jones, J. M. Lobert, I. A. Podgorny, J. M. Prospero, B. N. Holben, and N. G. Loeb, A model for the natural and anthropogenic aerosols over the tropical Indian Ocean derived from Indian Ocean Experiment data, J. Geophys. Res., 104, 27,421–27,440, 1999.

Savoie, D. L., J. M. Prospero, and R. T. Nees, Nitrate, nonsea-salt sulfate, and mineral aerosolover the northwestern Indian Ocean, J. Geophys. Res., 92, 933–942, 1987.

Sciare, J., H. Bardouki, C. Moulin, and N. Mihalopoulos (2003), Aerosol sources and their contribution to the chemical composition of aerosols in the Eastern Mediterranean Sea during summertime, Atmos. Chem. Phys., 3, 291–302, SRef-ID:1680 – 7324/acp/2003–3-291.

Smirnov, A., B. N. Holben, Y. J. Kaufman, O. Dubovik, T. F. Eck, I. Slutsker, C. Pietras, and R. N. Halthore, 2002b: Optical properties of atmospheric aerosol in maritime environments. *J. Atmos. Sci.*, **59,** 501–523.

Snirnov, and Coauthors, 2002a: Atmospheric aerosol optical properties in the Persian Gulf. J. Atmos. Sci., 59, 620–634.

Smirnov, A., B. N. Holben, T. F. Eck, I. Slutsker, B. Chatenet, and R. T. Pinker, 2002c: Diurnal variability of aerosol optical depth observed at AERONET (Aerosol Robotic Network) sites, *Geophys. Res. Lett.*, **29,** 23, 2115, doi:10.1029/2002GL016305.

Tanré, D., Y. J. Kaufman, M. Herman, and S. Mattoo: Remote sensing of aerosol properties over oceans using the MODIS/EOS spectral radiances, J. Geophys. Res., 102, 16,971–16,988, 1997.

Tindale, N. W., and P. P. Pease, Aerosols over the Arabian Sea: Atmospheric transport pathways and concentrations of dust and sea salt, Deep Sea Res., 46, 1577–1595, 1999.

Yu, H., Dickinson, R. E., Chin, M., Kaufman, Y. J., Holben, B. N. Geogdzhayev, I. V., and Mishchenko, M. I.: Annual cycle of global distributions of aerosol optical depth from integration of MODIS retrievals and GOCART model simulations, J. Geophys. Res., 108, 4128, doi:10.1029/2002JD002717, 2003.

Zdun, A., A. Rozwadowska and S. Kratzer, 2011. Seasonal variability in the optical properties of Baltic aerosols, Oceanologia, 53(1), 7-34.

Table 1. Correlation coefficients (R), mean bias, root mean squared error (RMSE) and the slope and intercept values of applied linear regression fits between MODIS and AERONET g_{aer} data. The statistical parameters are given separately for the pairs of wavelengths: (i) 470 nm (MODIS) and 440 nm (AERONET), (ii) 660 nm (MODIS) and 675nm (AERONET) and (iii) 870 nm (MODIS and AERONET). The statistical parameters are also given separately for winter, spring, summer and autumn. [a]

MODIS-Terra

		R	**Bias***	**RMSE**	**Slope**	**Intercept**
year	470-440	0.25	$2x10^{-4}$	0.045	0.36	0.45
	660-675	0.41	-0.028	0.060	0.55	0.32
	870	0.47	-0.035	0.070	0.60	0.29
Winter	470-440	0.20	$4.5x10^{-4}$	0.046	0.26	0.53
	660-675	0.35	-0.033	0.056	0.41	0.42
	870	0.41	-0.053	0.057	0.40	0.43
Spring	470-440	0.27	$-5x10^{-4}$	0.046	0.40	0.43
	660-675	0.44	-0.023	0.060	0.63	0.27
	870	0.50	-0.026	0.071	0.67	0.24
Summe	470-440	0.33	-0.002	0.044	0.51	0.35
	660-675	0.48	-0.031	0.061	0.71	0.22
	870	0.54	-0.030	0.077	0.79	0.16
Autumn	470-440	0.21	0.003	0.044	0.30	0.50
	660-675	0.33	-0.027	0.059	0.45	0.38
	870	0.41	-0.035	0.068	0.53	0.34

MODIS-Aqua

		R	**Bias***	**RMSE**	**Slope**	**Intercept**
	470-440	0.27	0.018	0.047	0.41	0.40
	660-675	0.42	-0.005	0.062	0.61	0.26
	870	0.46	-0.015	0.072	0.61	0.26
Win	470-440	0.25	0.024	0.049	0.36	0.43

[a]The reported correlation coefficients and slopes may be biased low, because we did not include in our analysis the unknown AERONET errors.

ter						
	660-675	0.39	-0.001	0.062	0.55	0.30
	870	0.43	-0.021	0.068	0.51	0.33
Spring	470-440	0.29	0.015	0.048	0.45	0.38
	660-675	0.45	-0.003	0.064	0.70	0.20
	870	0.50	-0.007	0.076	0.71	0.19
Summe	470-440	0.35	0.014	0.045	0.55	0.30
	660-675	0.50	-0.012	0.060	0.72	0.19
	870	0.53	-0.018	0.074	0.73	0.19
Autumn	470-440	0.20	0.021	0.047	0.30	0.47
	660-675	0.32	-0.003	0.061	0.46	0.36
	870	0.37	-0.014	0.069	0.48	0.34

* $g_{aer(AERONET)}-g_{aer(MODIS)}$

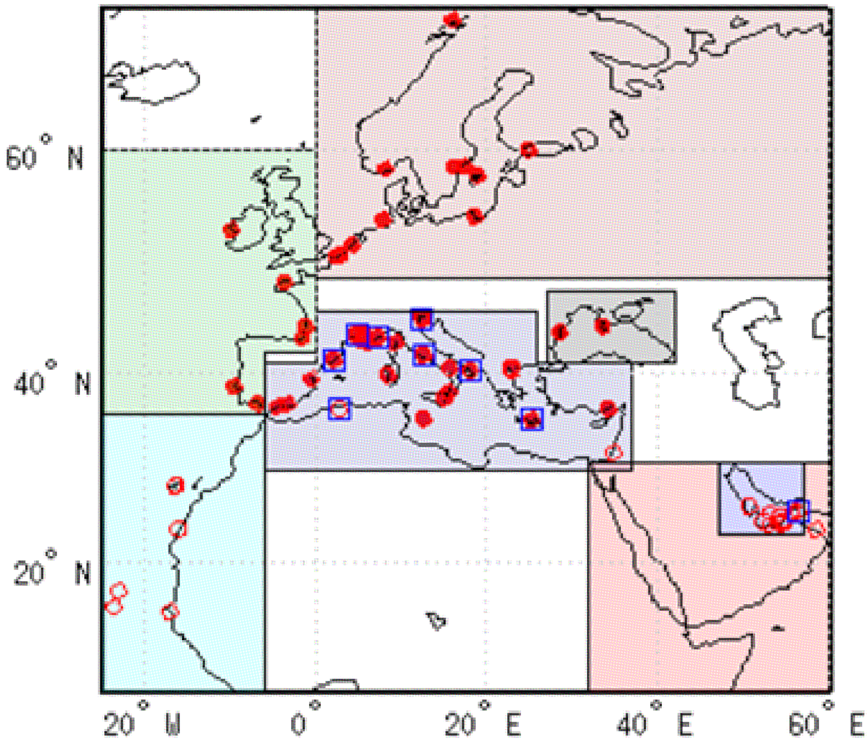

Figure 1. Comparison between HAC and MODIS total aerosol optical depth at 550nm. Global seasonal distribution of relative percentage differences ((HAC-MODIS)/MODIS -%) for: (a) winter (December-January-February), (b) spring (March-April-May), (c) summer (June-July-August) and (d) autumn (September-October-November). White shaded areas correspond to cases for which MODIS AOD values are missing or do not qualify for the averaging threshold.

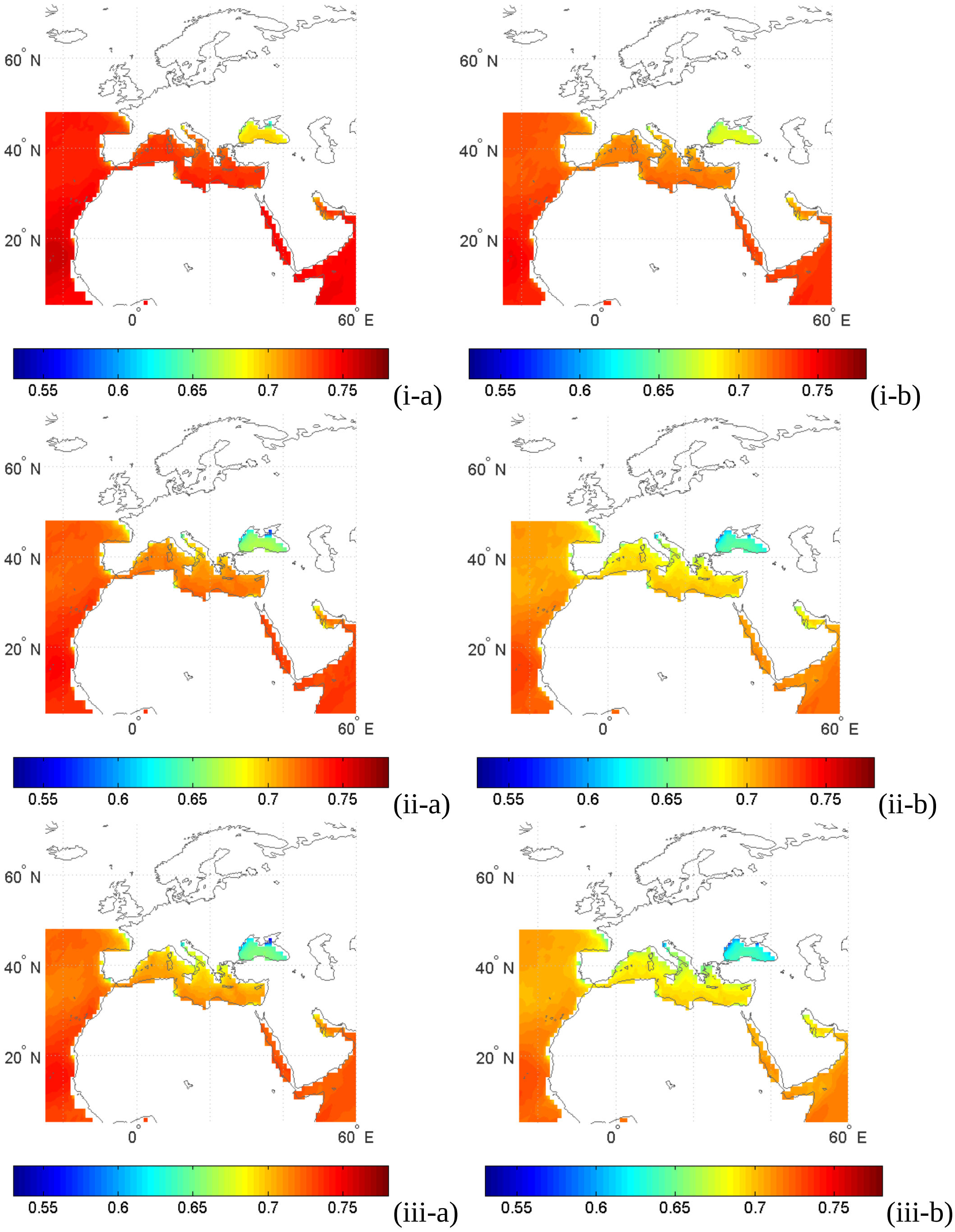

Figure 2. Geographical distribution of MODIS-Terra (-a, left column) and MODIS-Aqua (-b, right column) g_{aer} values averaged over 2002-2010, at the wavelengths of: 470 nm (i-, top row), 660 nm (ii-, middle row) and 870 nm (iii-, bottom row).

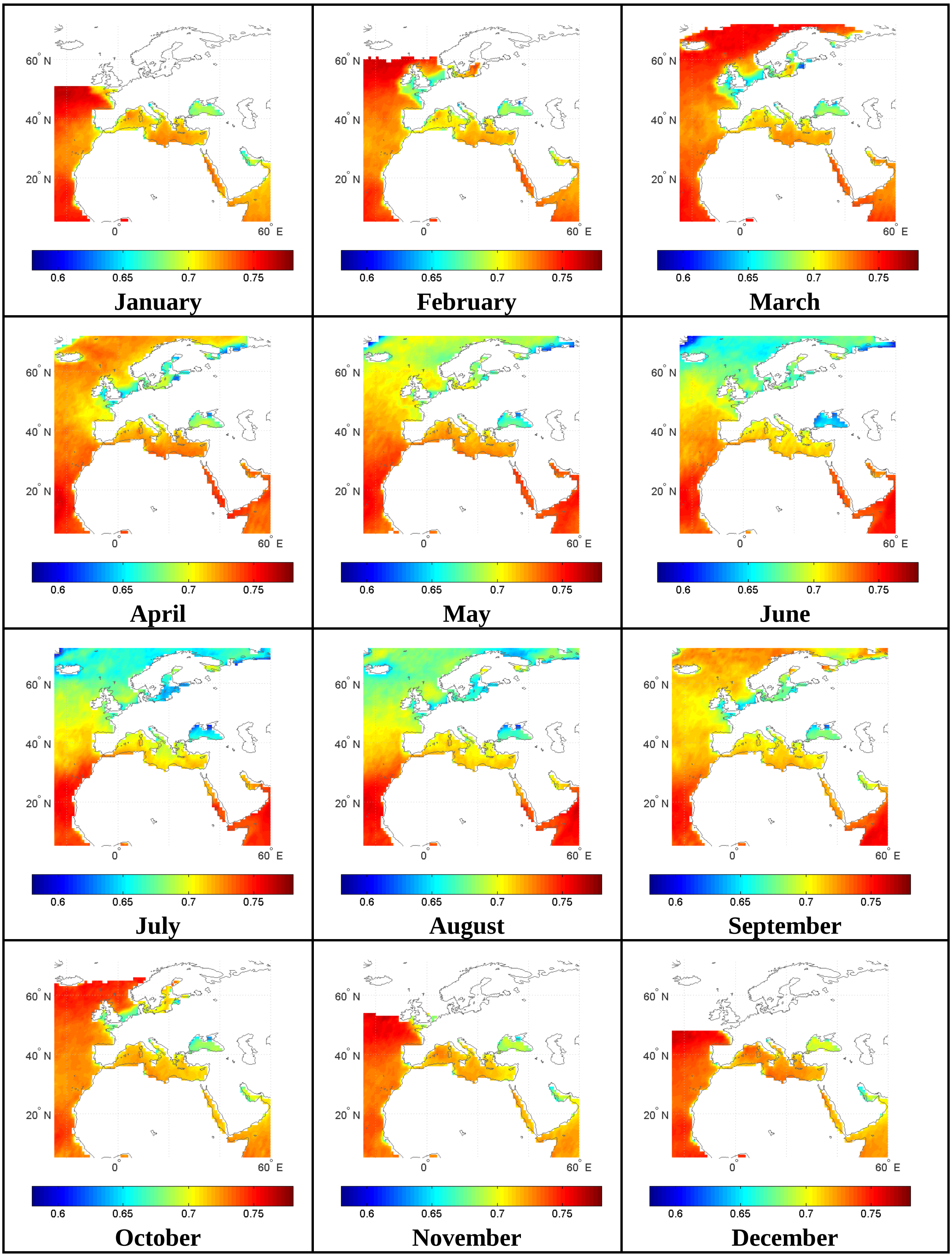

Figure 3. Month by month variation of MODIS-Aqua g_{aer} values at 470 nm averaged over the period 2002-2010.

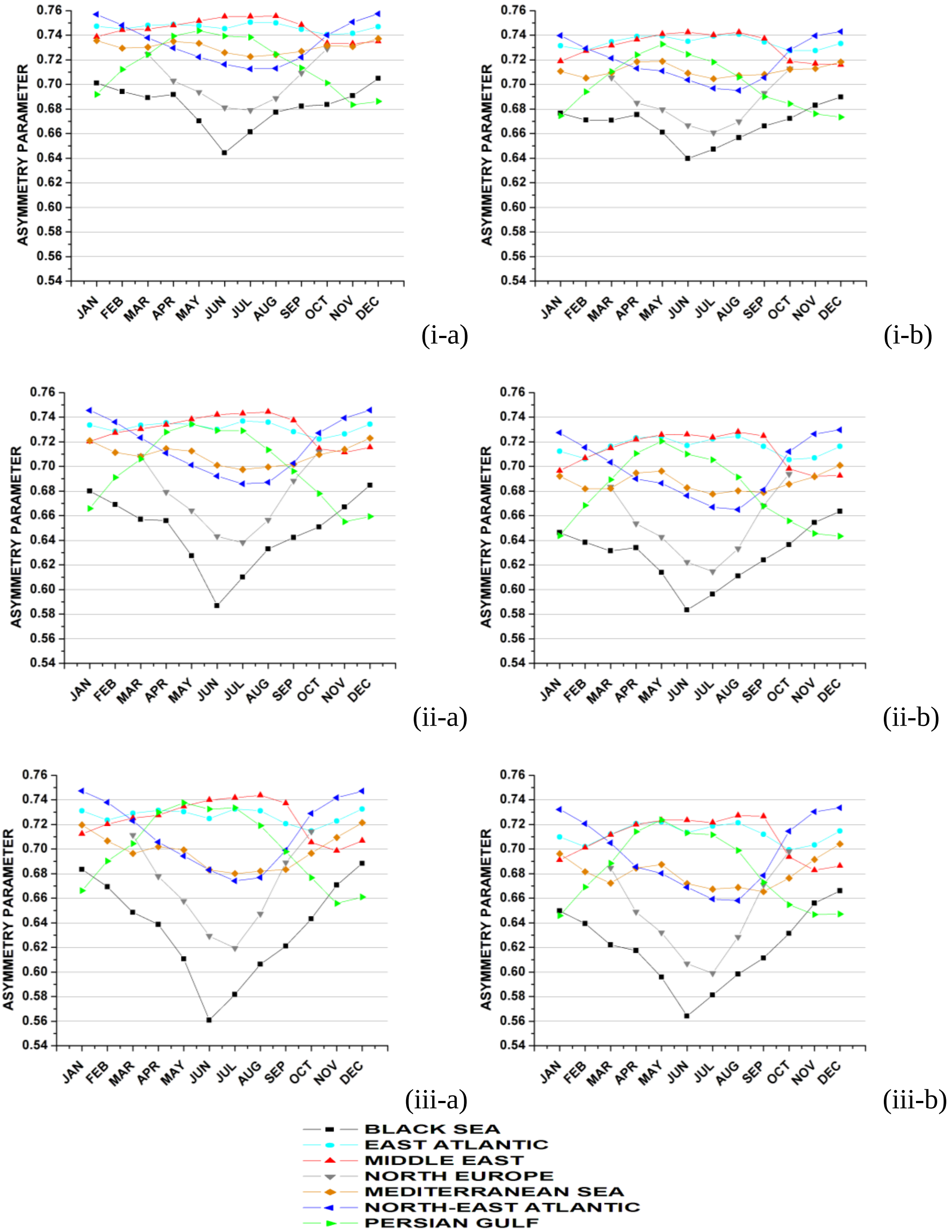

Figure 4. Intra-annual variation of MODIS Terra (-a, left column) and Aqua (-b, right column) g_{aer} values averaged over seven selected sub-regions (Fig. 1). Results are given for g_{aer} values at: 470 nm (i-, top row), 660 nm (ii-, middle row) and 870 nm (iii-, bottom row), averaged over the period 2002-2010, respectively.

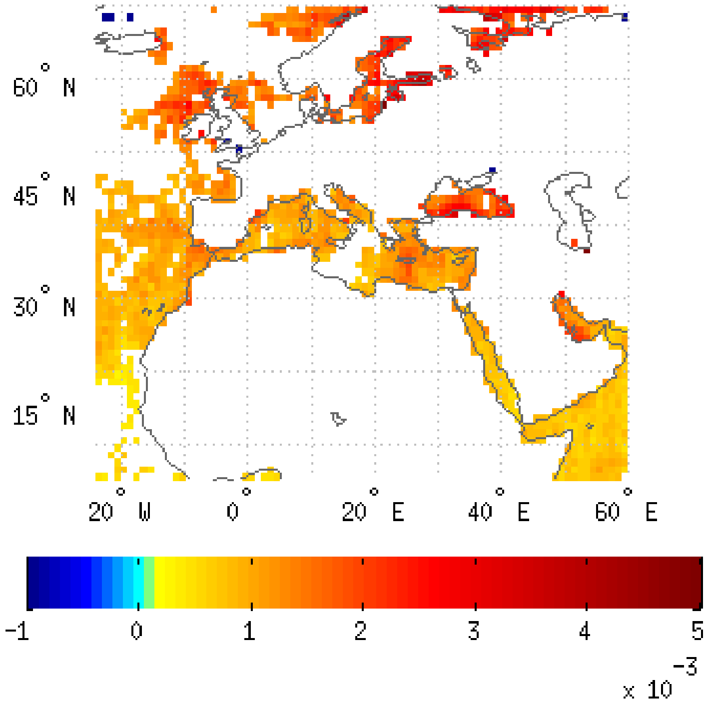

(a)

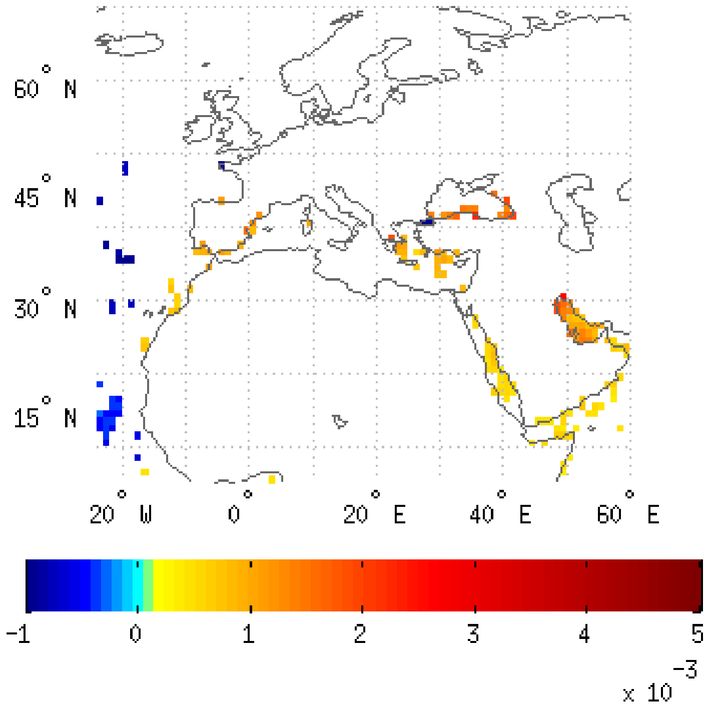

(b)

Figure 5. Slope (in units decade^{-1}) of MODIS g_{aer} deseasonalized anomalies over the period 2002-2010 from MODIS-Terra (-a, top) and MODIS-Aqua (-b, bottom), for the wavelengths of 470 nm.

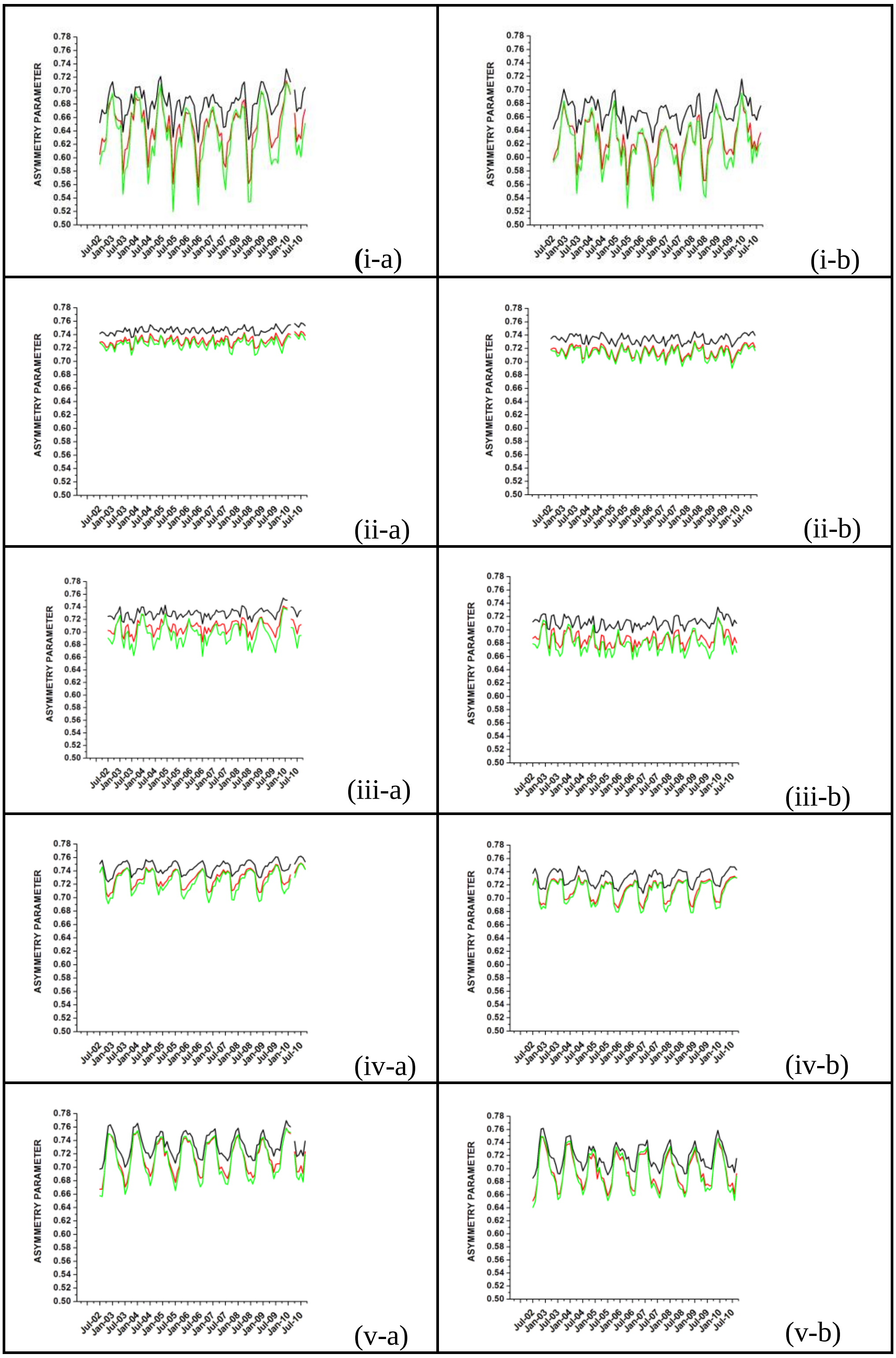

Figure 6. Inter-annual (2002-2010) variation of monthly mean g_{aer} values at 470 nm averaged over the sub-regions of: (i) Black Sea, (ii) Eastern Atlantic Ocean, (iii) Mediterranean Sea, (iv) Middle East, (v) North-eastern Atlantic Ocean, (vi) North Europe and (vii) Persian Gulf. Results are given based on MODIS-Terra (-a, left column) and MODIS-Aqua (-b, right column).

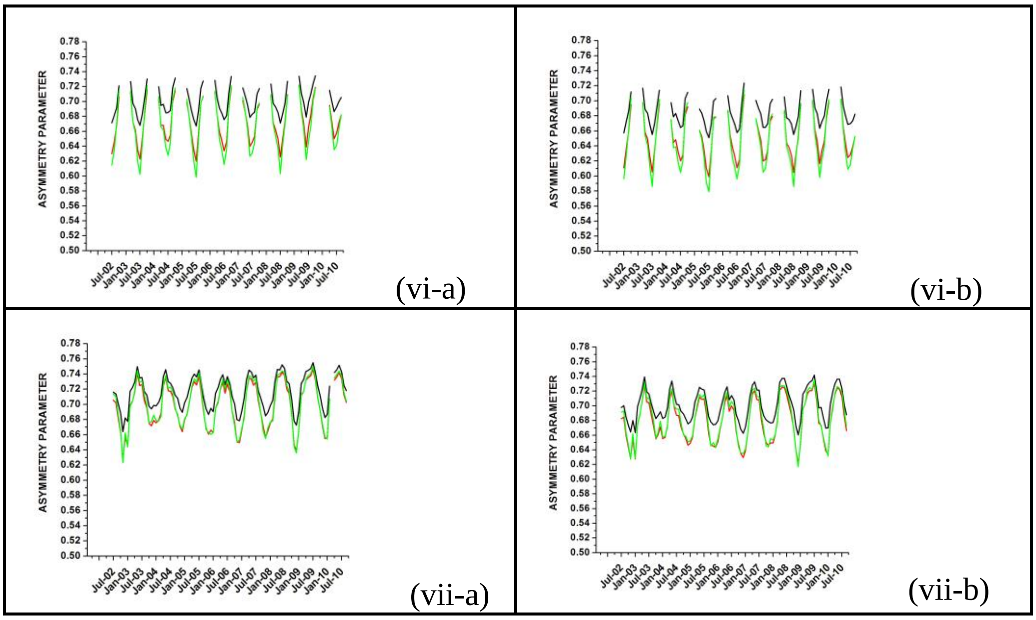

Figure 6 (continued). Inter-annual (2002-2010) variation of monthly mean g_{aer} values at 470 nm averaged over the sub-regions of: (i) Black Sea, (ii) Eastern Atlantic Ocean, (iii) Mediterranean Sea, (iv) Middle East, (v) North-eastern Atlantic Ocean, (vi) North Europe and (vii) Persian Gulf. Results are given based on MODIS-Terra (-a, left column) and MODIS-Aqua (-b, right column).

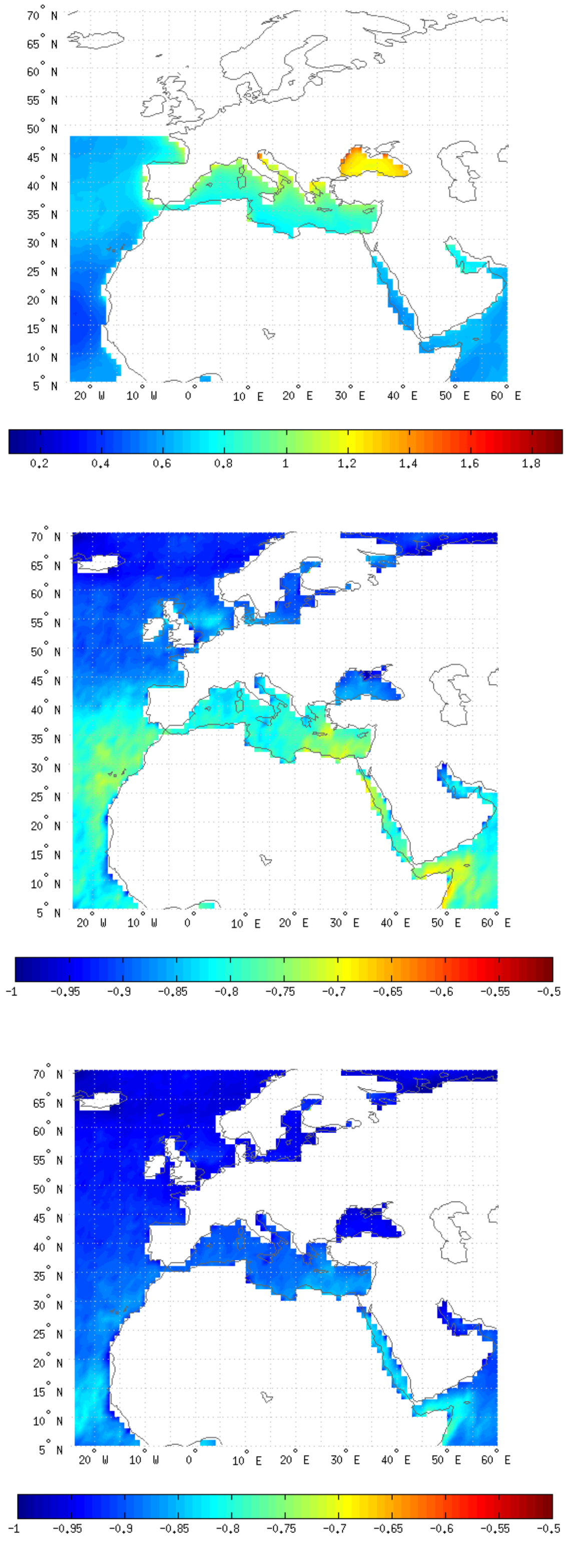

(a)

(b)

(c)

Figure 7. Geographical distribution of MODIS-Aqua C005 Angström exponent ($AE_{550-865}$) values averaged over 2002-2010, at the wavelength pair of 550-865 nm. The correlation coefficients between $AE_{550-865}$ and g_{aer} data at 660 and 870 nm are given in (b) and (c), respectively.

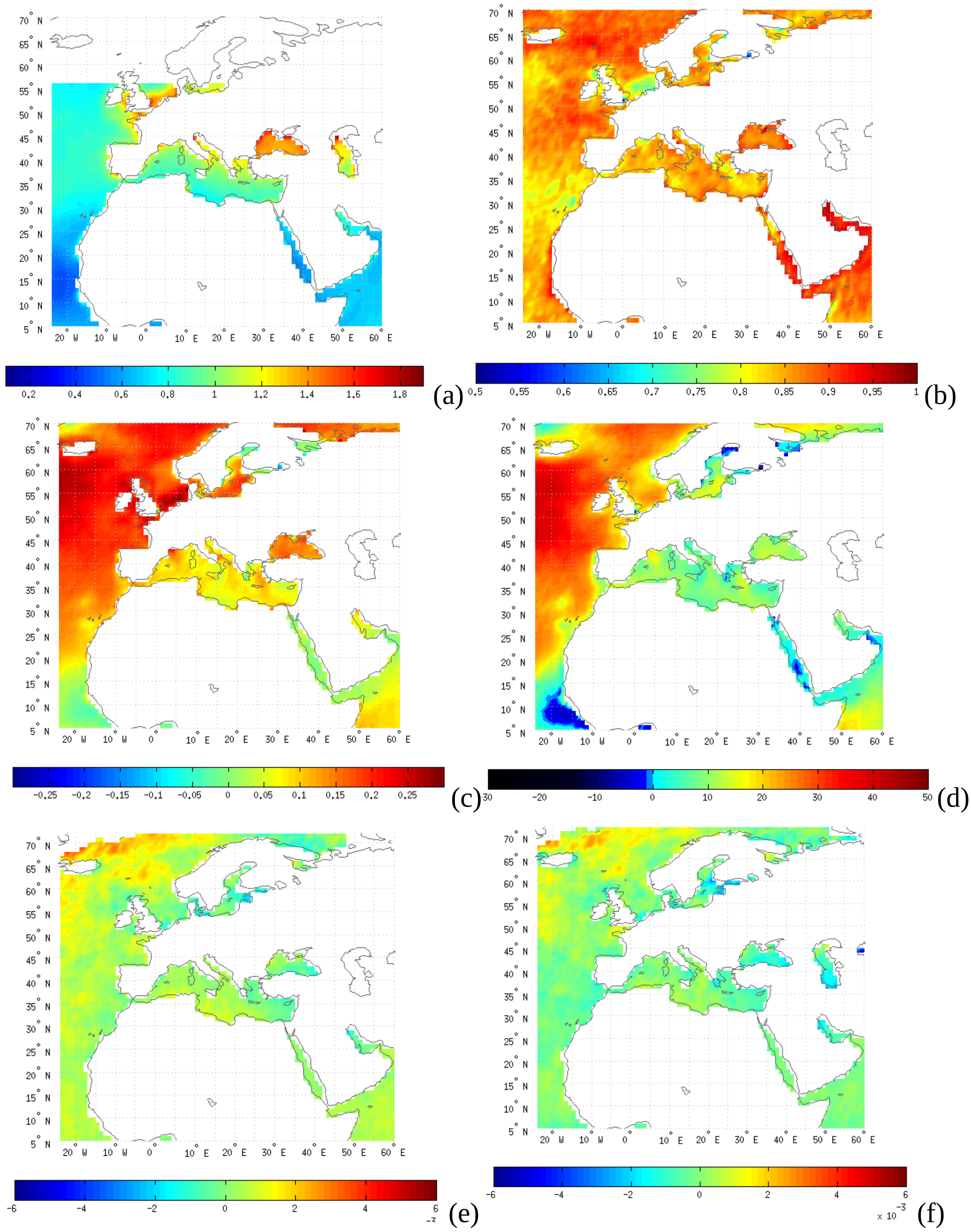

Figure 8. Geographical distribution of MODIS-Aqua C006 Angström exponent ($AE_{550-865}$) values averaged over 2002-2010, at the wavelength pair of 550-865 nm. In (b), (c) and (d) are given the correlation coefficients, the absolute biases and the relative percent biases, respectively, between the C006 and corresponding C005 AE_{550}-865 data. In (e) and (f) are given the computed deseasonalized trends of MODIS Aqua C005 and C006 $AE_{550-865}$) slope values for years 2002-2010, respectively.

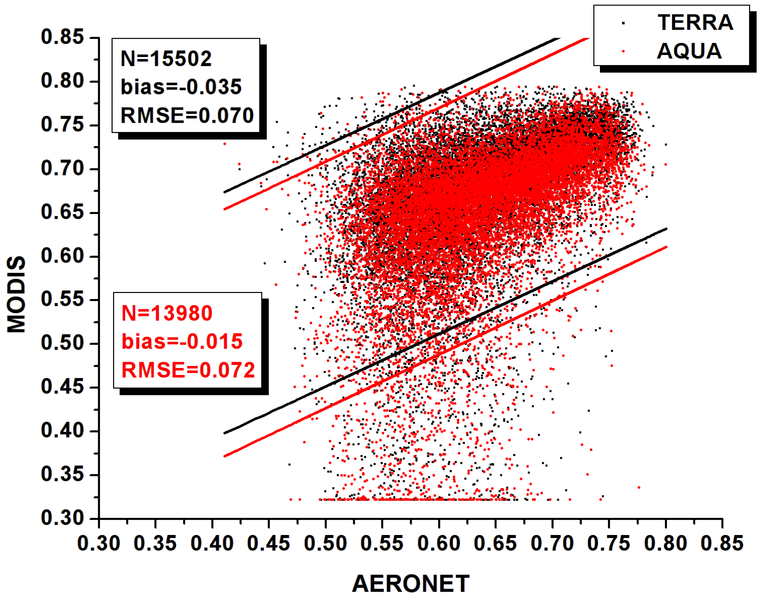

Figure 9. Scatterplot comparison between g_{aer} values at 870 nm from MODIS Terra (black color) and Aqua (red color) and corresponding values from AERONET stations (blue squares, Fig. 1). The 95% prediction bands as well as the mean bias and root mean squared error are given.

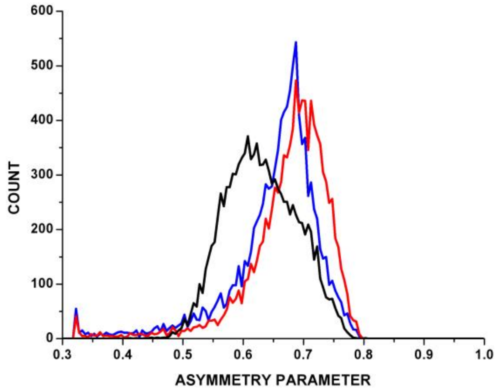

(a)

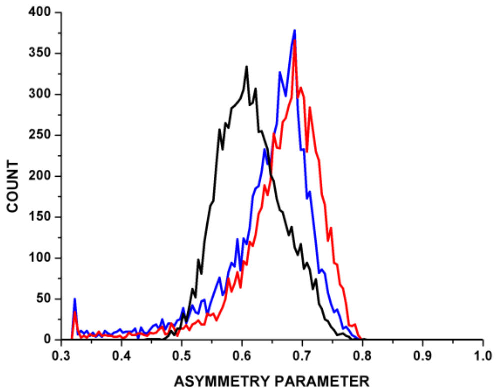

(b)

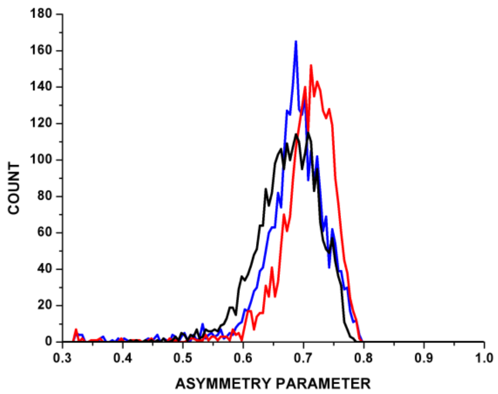

(c)

Figure 10. Frequency distribution histograms for MODIS-Terra (red colored lines) MODIS-Aqua (blue-colored lines) and AERONET (black lines) g_{aer} values at 870 nm. The histograms are given separately for: (a) the entire study region, (b) Europe and (c) Africa, Middle East and Arabian peninsula.

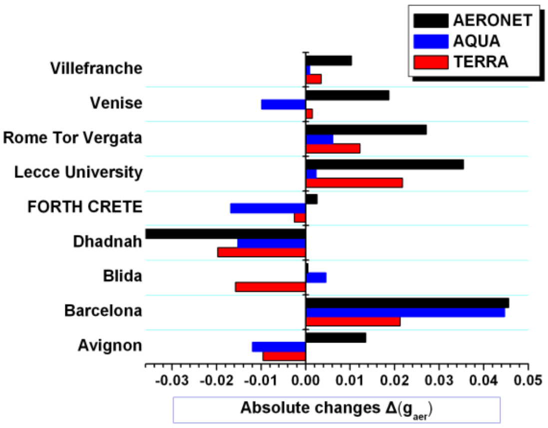

(a)

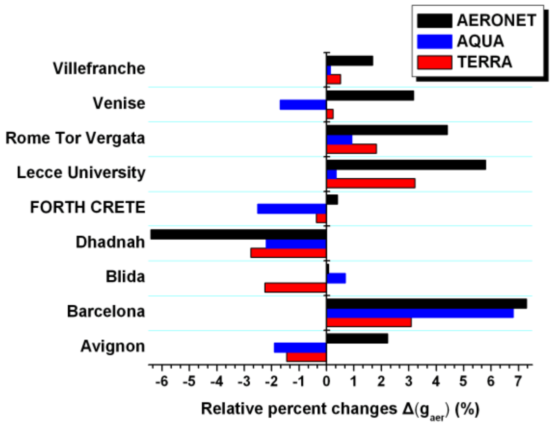

(b)

Figure 11. Frequency distribution histograms for MODIS-Terra (red colored lines) MODIS-Aqua (blue-colored lines) and AERONET (black lines) g_{aer} values at 870 nm. The histograms are given separately for: (a) the entire study region, (b) Europe and (c) Africa, Middle East and Arabian peninsula.

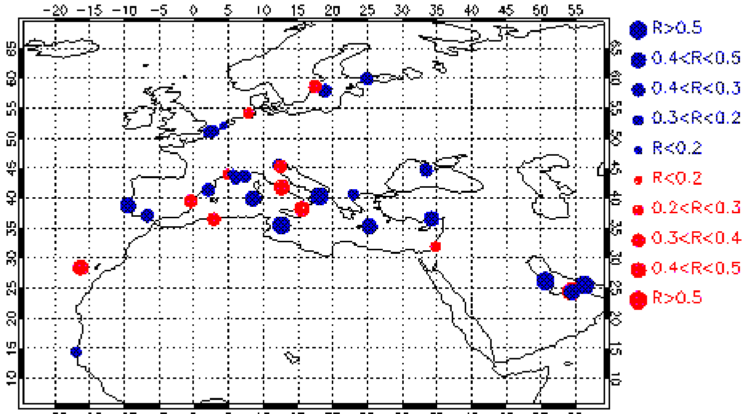

(a)

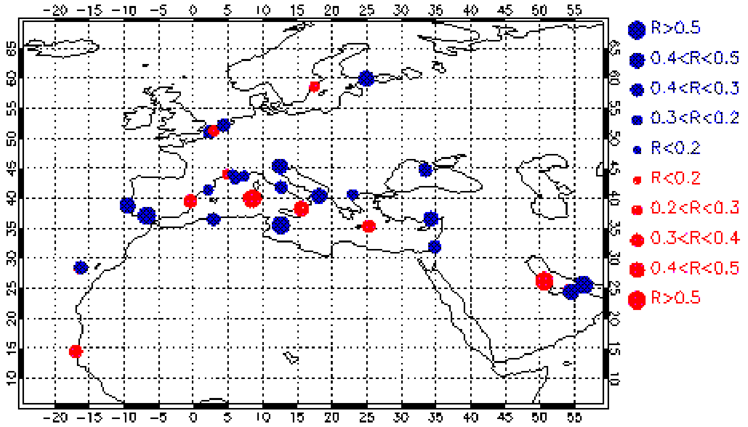

(b)

Figure 12. Map distribution of correlation coefficients between: (i) MODIS-Terra and AERONET g_{aer} values at 870 nm (left column) and (ii) MODIS-Aqua and AERONET g_{aer} values at 870 nm (right column). The size of circles corresponds to the magnitude of correlation coefficients, while blue and red colors are used for stations for which MODIS and AERONET indicate same and opposite tendency of g_{aer}, respectively.